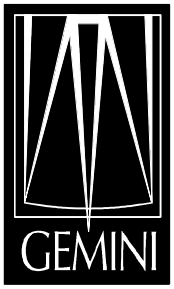

NEAR INFRARED FILTER BANDPASSES FOR GEMINI INSTRUMENTS

DOUG SIMONS
MARCH 1996

1.0 Purpose

Near-infrared filter bandpasses for use in future Gemini instrumentation is addressed in this technical note. This topic was first raised during informal discussions between the IfA, IRTF, and Gemini personnel during the summer of 1995. Soon thereafter the idea of modeling an infrared filter set for Gemini was proposed before the IRISWG and generally accepted as a useful step in the infrared instrument program. The September 1995 IRISWG also agreed that such an analysis should include both high altitude sites like Mauna Kea and lower altitude sites like Kitt Peak to determine if a single common bandpass specification could be achieved across a broad range of observatories. In the following note, the relatively simple technique used to define and characterize bandpasses is described. The intent is to reach consensus within Gemini through the IRISWG on a bandpass definition set, before defining filter fabrication specifications and polling the astronomical community to see if broad interest exists in the establishment of a common filter set for near-infrared astronomical use. Ultimately the IfA will coordinate the filter consortium that emerges from this activity since that institution is central to all of the Mauna Kea observatories and is building near-infrared instrumentation for several observatories over the next few years.

2.0 Analysis

Filter bandpasses were evaluated through MathCAD and a set of model atmospheres, provided by a number of sources. For Mauna Kea, a 1-6 μm model atmosphere generated by MODTRAN was kindly provided by Gene Milone. The model consists of atmospheric absorption at air masses of 1.0, 1.5, 2.0, 2.5, and 3.0 for an assumed 1 mm precipitable water vapor content at a 4200 m altitude location in the mid tropics. This absorption model was merged with a night sky emission model based upon the work of Roche and Glasse (1990, priv. comm.) to generate sky flux levels for the various bandpasses under consideration. Finally, Steve Lord at JPL kindly provided a model atmosphere for a 2 km altitude site, also at 1.0, 1.5, 2.0, 2.5, and 3.0 air masses. The MODTRAN and JPL models have very similar spectral resolution. No emission model was available for the low altitude site for this analysis, hence all sky backgrounds mentioned in this note apply directly to Mauna Kea and assume a telescope plus instrument emissivity of 3%, zenith pointing, and ambient temperature of 0 °C.

Filter curves were generated by convolving a simple Gaussian function with a box-car function of specified width. The convolution of these functions, with degrees of freedom specified in terms of bandpass width, central wavelength, peak transmission,

Bandpass	λ_c (μm)
J	1.24
H	1.65
K	2.20
L’	3.80
M’	4.67

Table 1 - Central bandpasses for all of the 1-5 μm atmospheric windows considered in this analysis are listed.

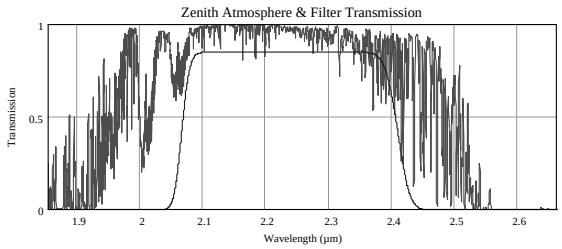

Figure 1 - A representative model bandpass plotted with Mauna Kea atmospheric transmission is shown.

and roll-off, offered good control over pertinent model factors and simulated the transmission curves of real filters fairly well. All filters were assumed to have a peak transmission of 85%.

Model bandpasses were generated by first estimating a central wavelength for each atmospheric window to define λ_c. For a fixed λ_c, peak transmission, and roll-off, the filters were allowed to expand in increments, $\Delta\lambda$, of typically ~0.03 μm for J, H, and K and ~0.08 μm at longer wavelengths. Table 1 lists the λ_c adopted for each atmospheric window. For each $\lambda_c \pm \Delta\lambda$ increment the following performance parameters were calculated:

- Sky background (under the aforementioned conditions) in terms of magnitudes per arcsec^2 and photons/arcsec^2/sec at the Gemini focal plane

- Non-linearity of photometric extinction, σ, in the 1.0-3.0 air mass range for Mauna Kea and a 2 km altitude site. Here, σ is defined as the standard deviation of the set fit_i - $(-2.5log(\tau_i))$ where fit_i is a linear least squares fit to the log of the atmospheric transmission τ_i. The parameter σ is therefore an estimate of the photometric error contribution in magnitudes.

- The zenith absorption, τ_0, for both the Mauna Kea and 2 km site, defined as

$$\tau_0 = \frac{1}{\Delta\lambda}\int_{\lambda_1}^{\lambda_2} f(\lambda)\tau(\lambda)d\lambda$$

where $f(\lambda)$ is the filter function, $\tau(\lambda)$ is the atmospheric absorption at zenith, λ_1 and λ_2 are the ~10% transmission points in the filter profile and $\Delta\lambda=\lambda_2-\lambda_1$. The parameter τ_0 is therefore the mean value of the product $f(\lambda)\tau(\lambda)$ across $\Delta\lambda$ and gauges when further broadening of a proposed bandpass no longer leads to increased flux through a filter.

Figure 1 shows a typical prototype filter bandpass used in the investigation of the K-band. Also shown is the Mauna Kea zenith atmospheric absorption. Figure 2 shows the corresponding extinction linearity analysis for this bandpass. The line represents a least squares fit to the extinction measured between 1 and 3 air masses. Figure 3 shows the sky emission for this spectral region which was used in conjunction with the filter bandpass to estimate sky background levels for each $\Delta\lambda$ increment in the analysis.

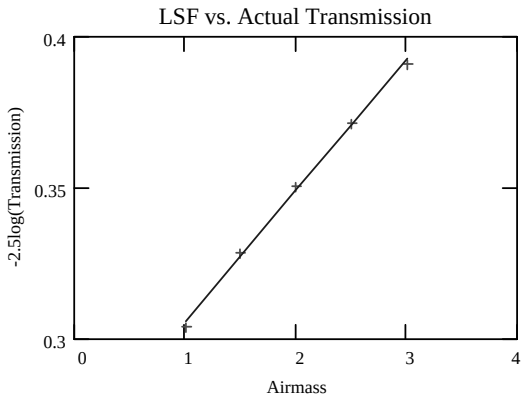

Figure 2 - Crosses denote model transmission of the filter and atmosphere shown in Figure 1. The line is a least squares fit.

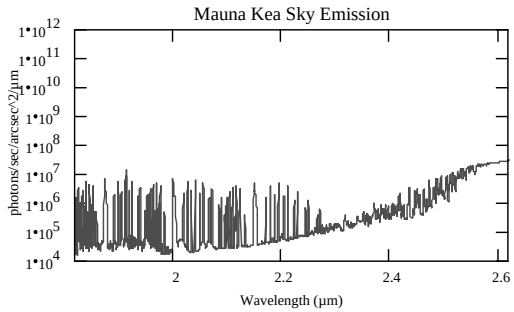

Figure 3 - Model sky emission above Mauna Kea is shown for the K-window. A combination of OH lines and thermal flux defines the emission. This includes a 3% ε telescope contribution.

3.0 Proposed Bandpasses

A number of optimization strategies can be used to define near-infrared broadband filters. For example, Young, Milone, and Stagg (1994, *A&AS*, **105**, 259) conducted a detailed study of the JHKLMNQ bands by defining a figure of merit for the linearity of extinction curves for various sites under various water vapor conditions. Bandpasses were optimized primarily on the basis of reproducibility and transformability of photometric measurements across various sites.

The approach adopted here was to assess extinction linearity, throughput, and background flux for possible bandpasses in a *simple* manner. Unlike Young *et al*. (1994), total throughput (atmosphere + filter) was heavily weighted in the optimization process, not just photometric performance, on the assumption that most astronomical applications demand peak S/N even if it means a few percent degradation in photometric accuracy. The result is a set of bandpasses that are considerably broader than the triangular shaped highly optimized bandpasses derived by Young et al. (1994), resulting in increased throughput but still fairly good photometric performance.

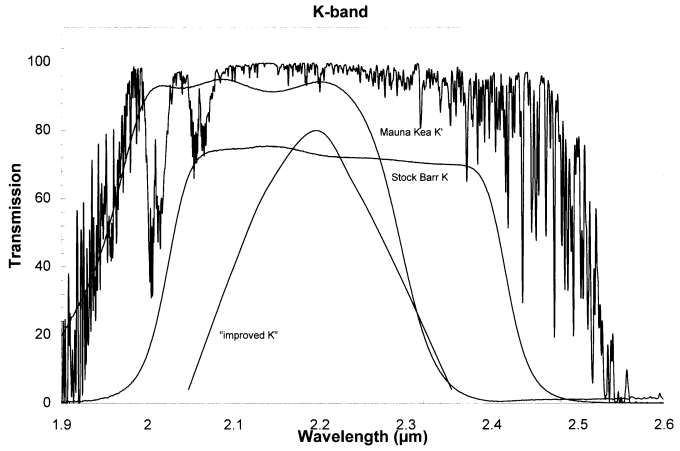

Figure 4 - The atmospheric K window is plotted together with the Young *et al*. "improved K" filter, which has a triangular shape and has been tuned to deliver optimal photometric accuracy, albeit at the expense of throughput. Also plotted are scans of the Redeye stock K and K' filters.

As a "sanity check" proposed filters were also compared with stock Barr JHKLL'M filters to determine if there is any real gain to be had from changing from this commonly used set. Table 2 lists the filter sets in use now at several observatories on Mauna Kea, including those in NSFCAM (IRTF), IRCAM3 (UKIRT), and Redeye (CFHT), as well as the Barr set to

illustrate filter commonality between these observatories.

Filter	Barr λ_1-λ_2 (µm)	UKIRT λ_1-λ_2 (µm)	IRTF λ_1-λ_2 (µm)	CFHT λ_1-λ_2 (µm)
J	1.11-1.39	1.13-1.42	1.11-1.42	1.10-1.39
H	1.50-1.80	1.53-1.81	1.48-1.76	1.51-1.79
K	2.00-2.40	2.00-2.41	2.02-2.41	2.02-2.41
K’			1.95-2.29	1.95-2.29
K_s		1.99-2.32	1.99-2.31	
L	3.20-3.80	3.15-3.75	3.20-3.81	
L’	3.50-4.10	3.50-4.10	3.49-4.08	
M	4.50-5.10		4.54-5.16	
M’		4.55-4.80	4.67-4.89	

Table 2 -Bandpasses for stock near-infrared filters at 3 observatories and Barr Associates are listed to demonstrate commonality of filters across several Mauna Kea observatories.

Plotted in the following pages are Barr and proposed filter bandpasses for the JHKLM windows. All filter curves have been plotted with the Mauna Kea model atmosphere for 1.5 air masses to illustrate how the filters “fit” within windows. Also shown in the upper right panel of each page is σ (in millimag) and τ_0 as a function of filter bandpass for Mauna Kea and a 2 km altitude site. A vertical dotted line corresponds to the proposed bandpass at the ~10% transmission level in the filter profile. In general the bandpass was selected on the basis of when total throughput (τ_0) begins to fall and photometric error (σ) over the 1.0-3.0 airmass range begins to rise rapidly with increasing $\Delta\lambda$. Also shown for each window is the Mauna Kea zenith atmosphere plus telescope emission. This plot is not included in the J-band plots because the model only covers $\lambda > 1.45$ µm.

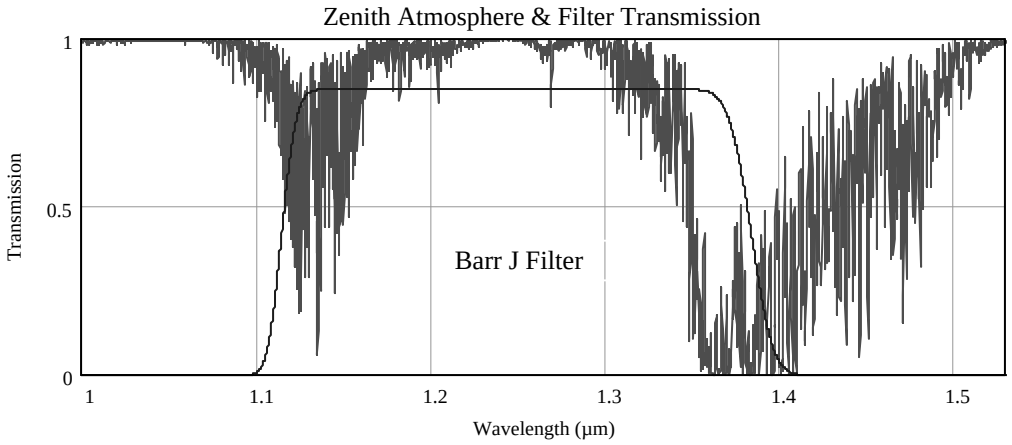

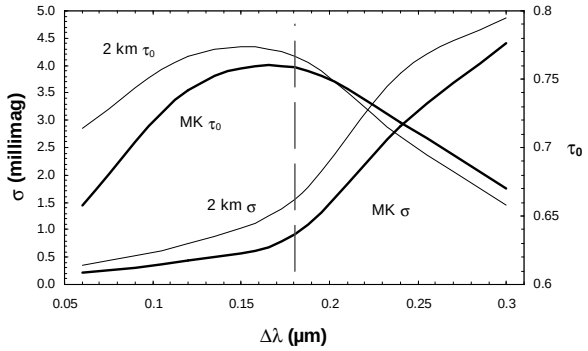

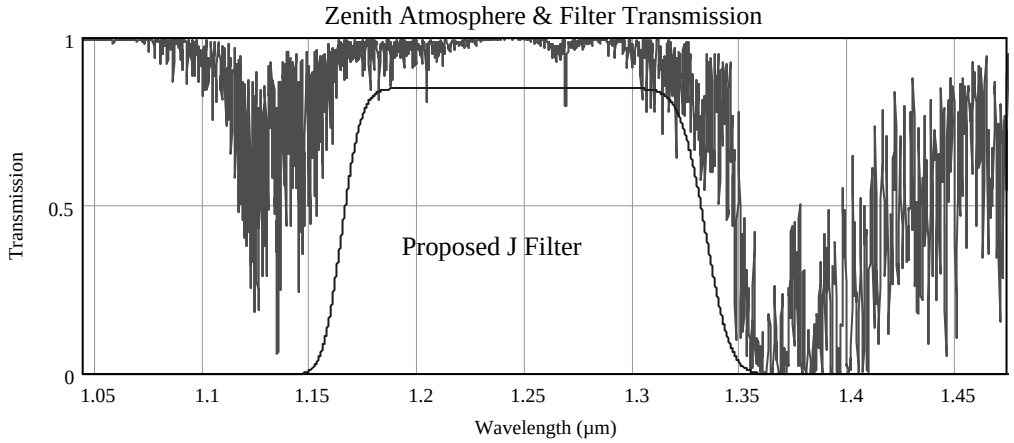

Comments: The commonly used J-band filter, plotted at top, is clearly a poor match to the atmosphere. Nearly 50% of the bandpass covered by the Barr filter is contaminated by water vapor lines, leading to a ~5x greater photometric error contribution than the proposed bandpass. Furthermore, the J window is heavily populated with OH emission lines which are needlessly passed through the oversized Barr filter bandpass. The net result is significantly increased sky background (~0.5 magnitudes) and photometric error over the proposed bandpass.

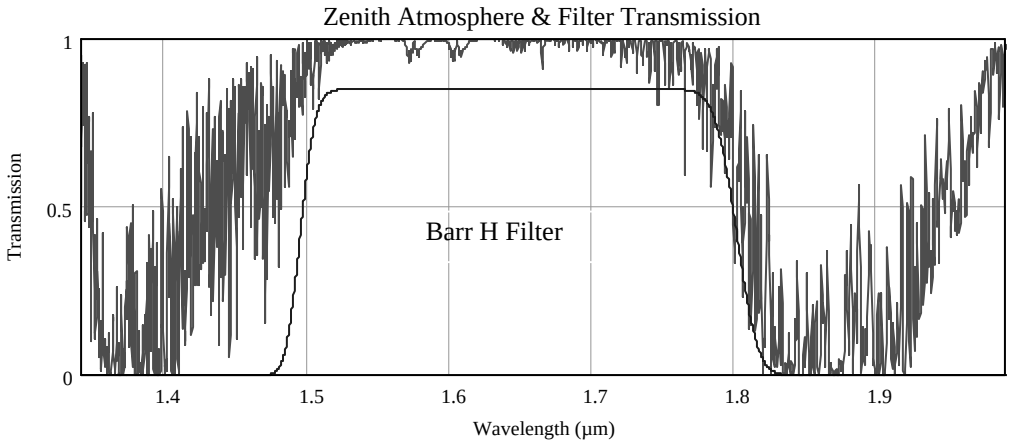

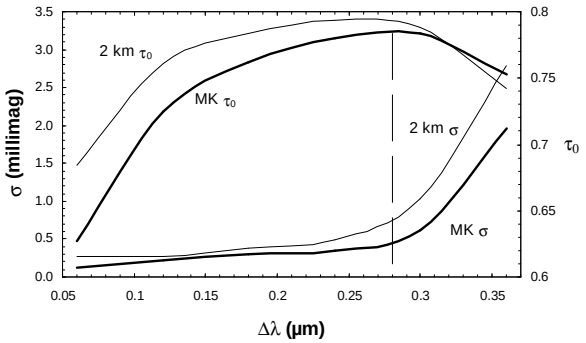

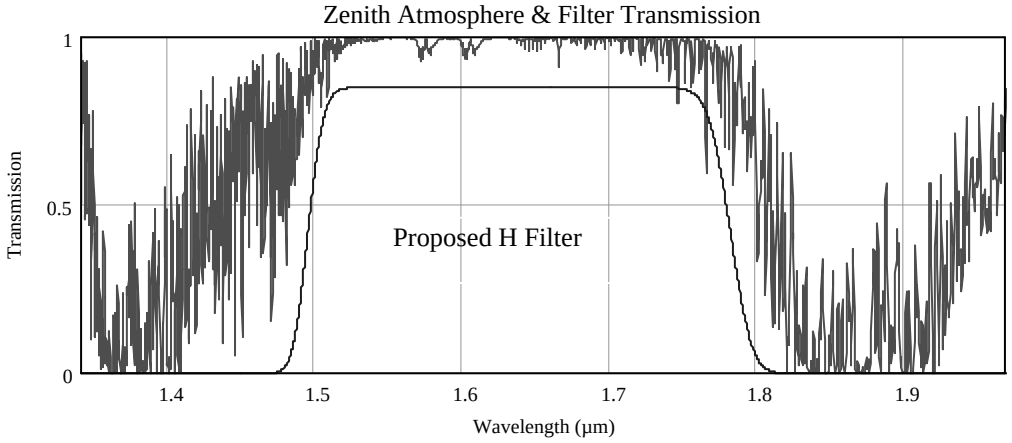

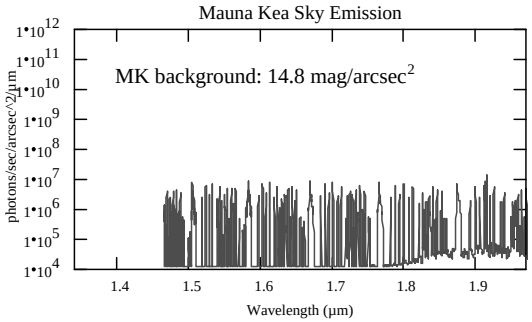

Comments: The Barr H filter intrudes slightly into the water vapor band near 1.80 μm but is otherwise a reasonably good fit to this window. To the upper right the photometric error is seen to rise dramatically for bandpasses greater than ~0.30 μm, leading to the proposed H filter which has a width slightly under 0.30 μm.

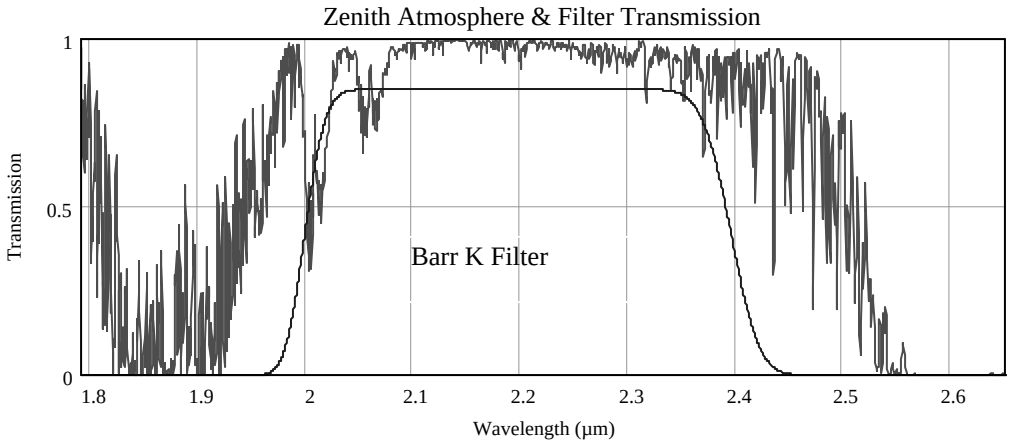

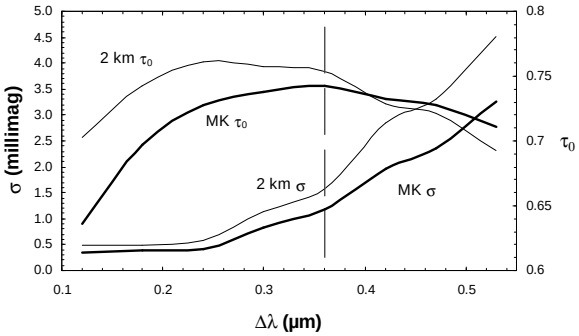

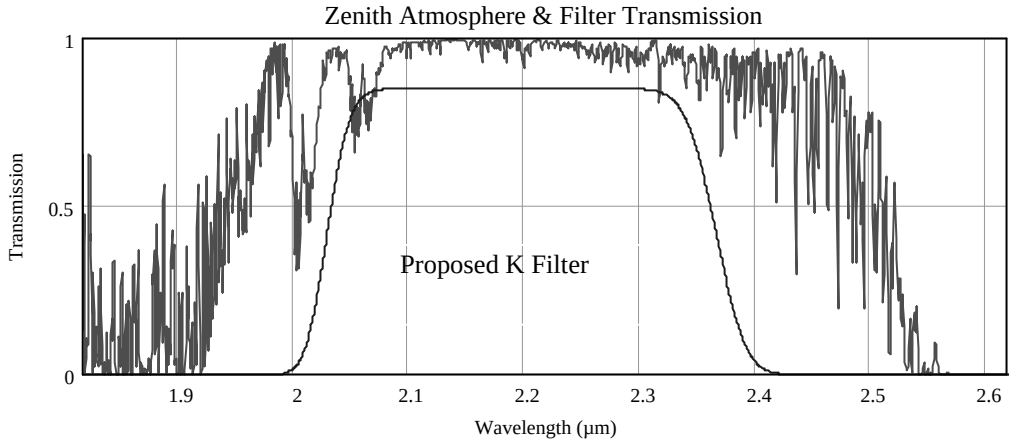

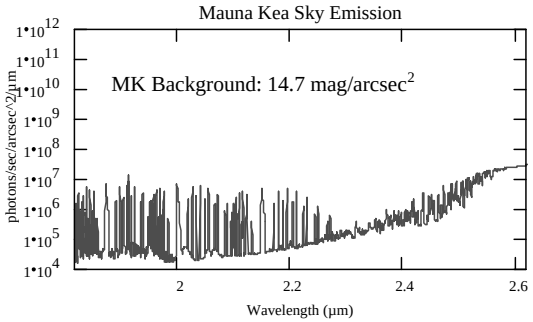

Comments: Like the Barr H filter, the Barr K filter is a reasonably good fit to the 2.2 μm atmospheric window. Photometric performance is effected by the strong CO_2 lines at 2.01 and 2.06 μm. The impact of these CO_2 lines on delivered photometric noise is seen in the plot of σ above, where bumps in the σ plot corresponding to $\Delta\lambda \sim 0.30$ and 0.42 μm are seen. The proposed K filter is slightly narrower and is designed to avoid the strong CO_2 line at 2.01 μm, providing improved photometry compared to K', K_s, or the Barr K filter.

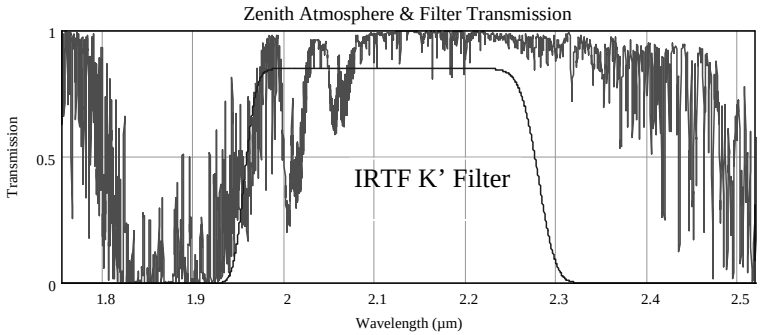

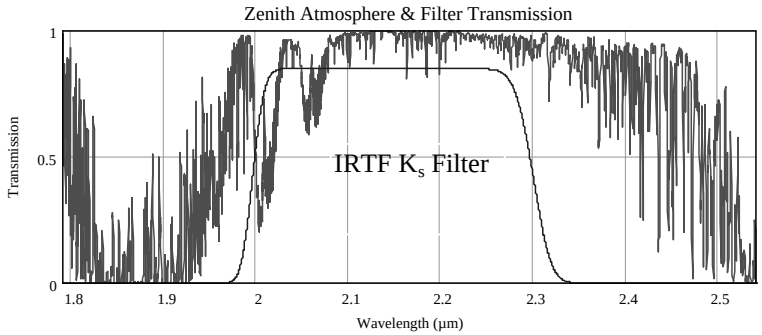

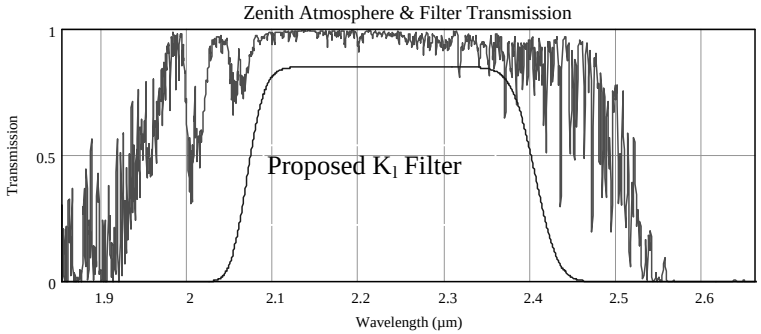

Comments: Specialty filters within the K window are shown. The K' filter covers shorter wavelengths than K_s, hence is more susceptible to water vapor impacting performance than K_s. A different filter dubbed K_{long} is proposed which takes advantage of Gemini's low emissivity and avoids the deep CO_2 absorption lines at 2.01 and 2.06 μm. No significant increase in sky background would result from such a bandpass while throughput and extinction linearity would be improved over K_s and K'. The overall performance of K_{long} is similar to the proposed K filter since both avoid the deep CO_2 lines and have comparable width. Since this filter is tuned for low emissivity telescopes, the advantages it theoretically offers may not be easily applicable to other telescopes and warmer sites.

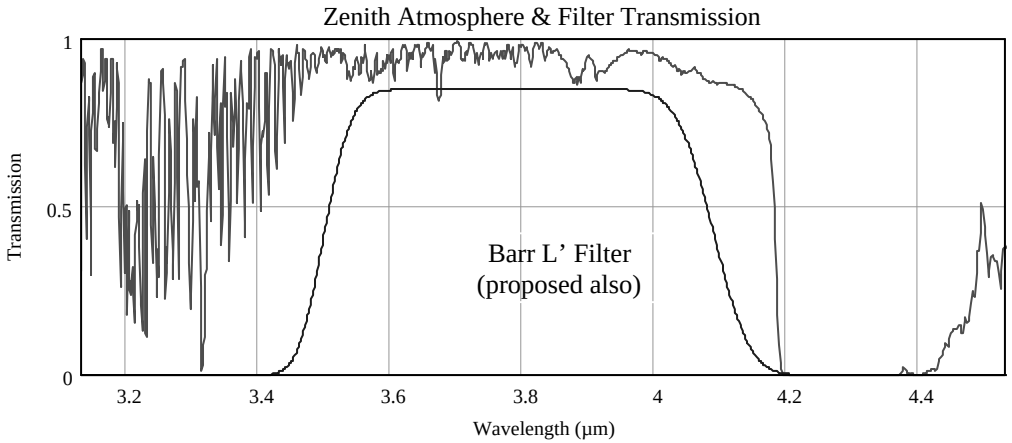

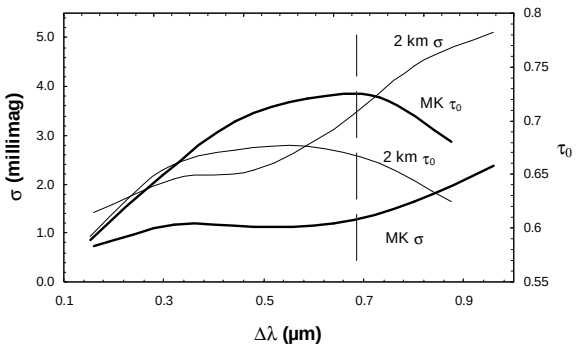

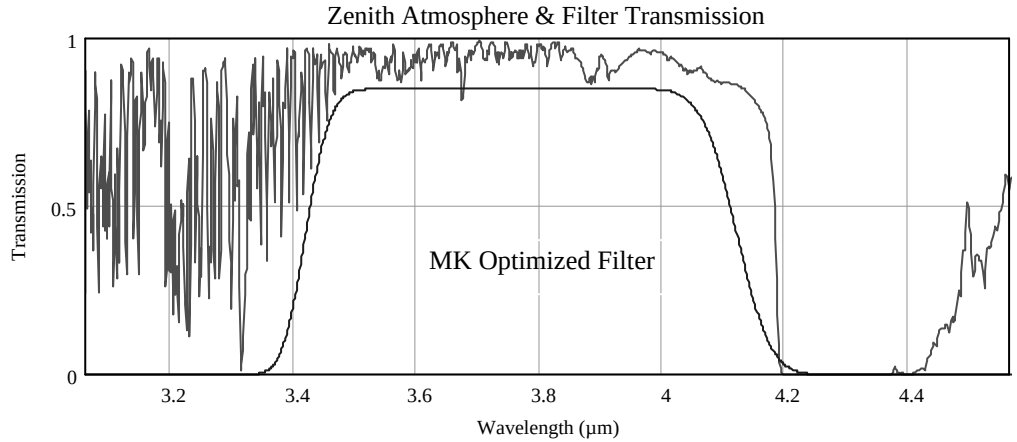

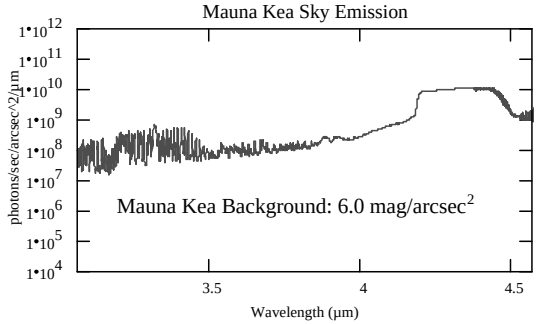

Comments: Since the red (high emissivity) end of the ~4 μm window is also clear of telluric lines, simultaneously optimizing this bandpass for low background and good photometric performance is difficult. The "MK Optimized" L' bandpass corresponds to the roll-off transmission point for both the Mauna Kea and 2 km sites, as seen in the upper right plots. In the Mauna Kea case, no significant boost in σ from this wider bandpass is created, as the σ plot is nearly flat up to the bandpass proposed. The 2 km σ is nearly a factor of 3 worse for this bandpass though. The Barr L' bandpass offers a reduced background and is a better compromise between the MK and 2 km cases.

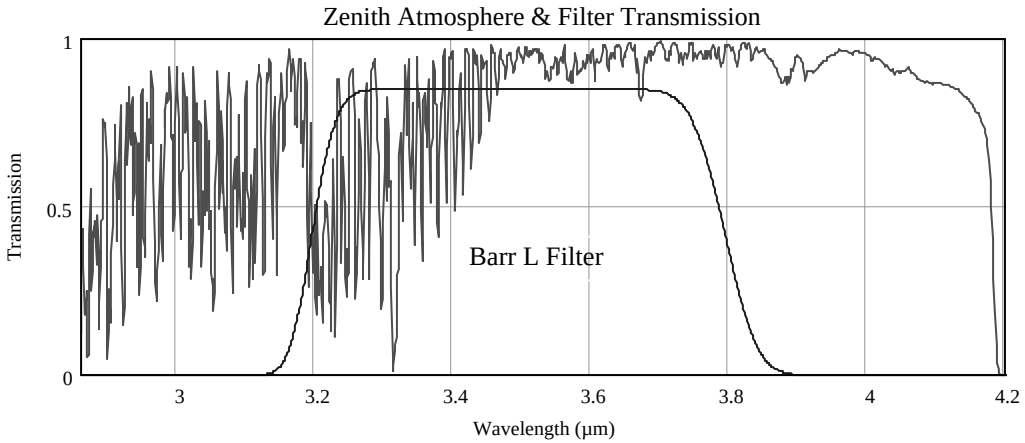

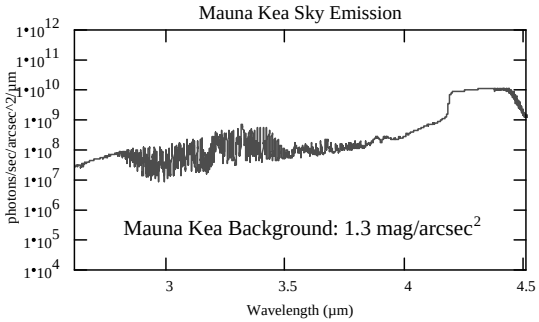

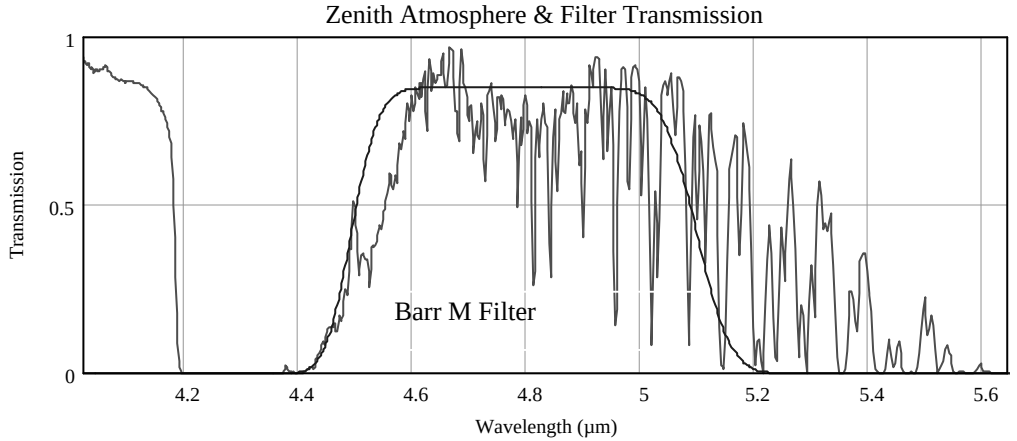

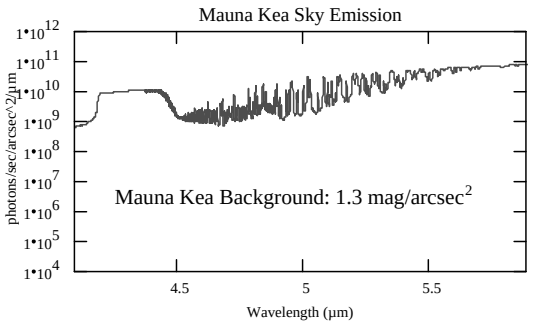

Comments: The Barr L and M filters are shown, both of which are heavily contaminated by telluric lines. No substitute for these filters is proposed here because the proposed L' and M' filters are logical replacements for L and M.

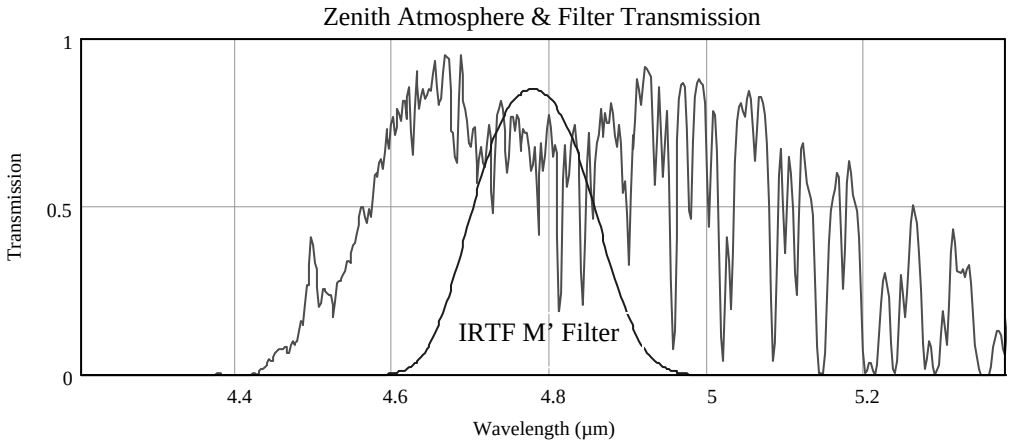

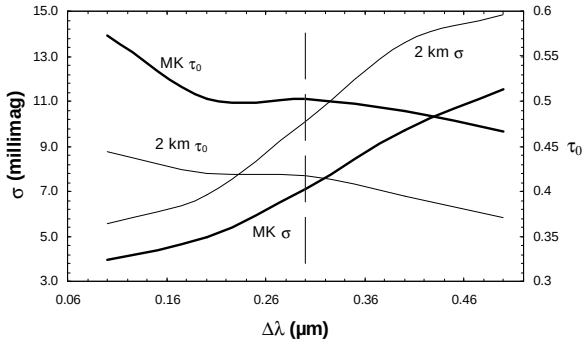

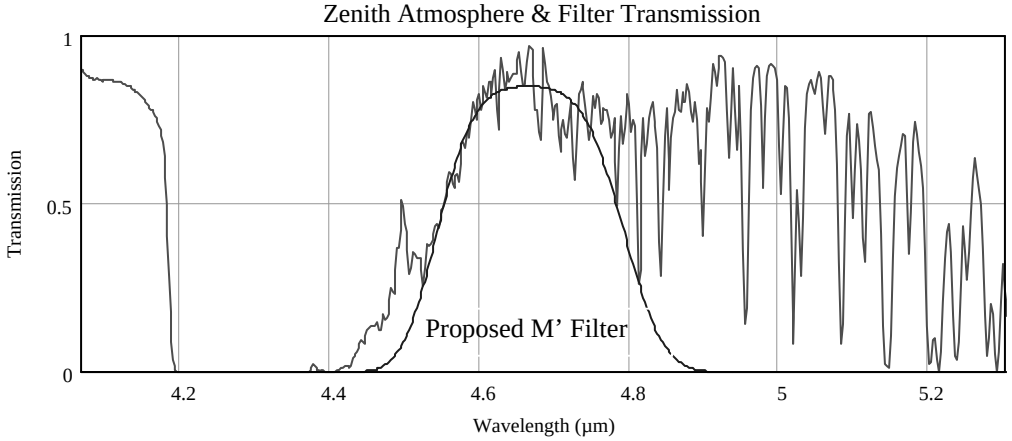

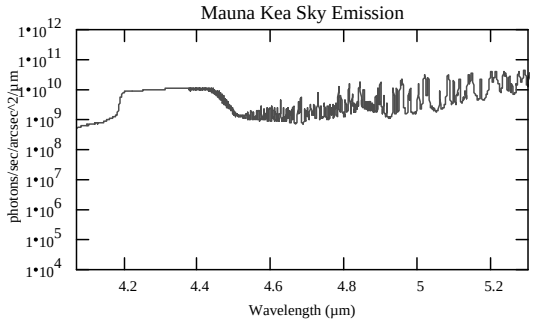

Comments: The IRTF M' filter suffers from several absorption lines, leading to an estimated photometric error of ~8 millimag when used on Mauna Kea and ~10 millimag on a 2 km altitude site. The proposed filter is shifted significantly bluer, into a more transparent region within the M window, which also offers significantly lower background, boosting overall S/N. The proposed filter is actually close to the nbM filter in use at UKIRT and has a theoretical photometric error contribution of ~7 millimag on Mauna Kea. Like the L' filter, a significant difference exists in the photometric performance of such filters when used on Mauna Kea and a 2 km altitude site, making it difficult to select a single bandpass that is well suited for both mid and high altitude sites.

4.0 Conclusions

Table 3 summarizes key performance levels and bandpass definitions for the Barr and proposed new filters. All but one proposed bandpass (L') provides improved photometry and reduced background over the Barr set with no loss in effective throughput. In some cases, the difference between existing filters and new ones is small but in all cases the proposed bandpasses meet or exceed the performance of commonly used Barr filters. In the case of the J filter, the proposed bandpass will no doubt lead to significantly improved photometry and signal-to-noise (due to the ~0.5 mag reduced background), with no real loss in effective throughput since so much of the Barr J filter is heavily obscured by water vapor absorption. In general, not surprisingly, lower photometric errors will be achieved on Mauna Kea than lower altitude sites, but at least at J, H, and K, the differences should be quite small for the proposed bandpasses. The L' filter in particular represents a difficult set of trades. The ~4 µm window is relatively clear of telluric lines at the red (high emissivity) end of the window, hence simultaneously minimizing the effect of atmospheric absorption and emission is difficult. Ultimately the signal-to-noise achieved for science targets is a function of the color of the target, which can range from stellar (peak flux short of ~4 µm) to dust (peak flux beyond ~4 µm), hence weighting the location of λ_c on the blue end of this window to cut the background will not necessarily lead to the highest signal-to-noise for all sources. The best compromise between competing factors is the Barr L' filter, which is narrower than the proposed bandpass (hence lower background), centered in the window (does not favor a particular color source), and offers better 2 km site performance than the "MK Optimized" filter. No suggested changes are offered here to the L and M Barr filters, because these obsolete bandpasses are logically replaced by the L' and M' filters anyway. The IRTF M' filter does not appear to be well matched to the ~5 µm atmospheric window and this analysis favors a filter closely resembling that already in use at UKIRT (nbM in IRCAM3), which offers a lower background and better extinction linearity than the IRTF M' filter. A new specialty K filter is proposed, dubbed K_{long}, which on Gemini offers improved throughput and photometry over K_s or K' with no increase in background, no doubt due to the low emissivity of the Gemini telescopes. The gains of such a filter may not be achievable on other telescopes with higher emissivities, hence expecting it to be broadly accepted as a new standard filter at other observatories seems unlikely. Still, the gains of K_{long} at Gemini are real and this filter should be considered as part of Gemini's standard filter set. Finally, in no case is the background in the proposed filters prohibitively high for Gemini's NIRI. Even in its wide field mode (0.12 arcsec pixels) with modest read rates (few fps), the background delivered by these filters can be tolerated.

Name	Proposed Filters						Barr Filters					
		Mauna Kea			2 km			Mauna Kea			2 km	
	Bandpass♣ (μm)	τ_0 (%)	σ (millimag)	Sky (γ/sec/as^2)	τ_0 (%)	σ (millimag)	Bandpass♣ (μm)	τ_0 (%)	σ (millimag)	Sky (γ/sec/as^2)	τ_0 (%)	σ (millimag)
J	1.17-1.33	76	1.0	~4e4♠	77	1.6	1.11-1.39	66	4.6	~8e4♠	65	5.1
H	1.49-1.78	79	0.6	4.8e5	79	0.9	1.50-1.80	78	0.9	4.9e5	78	1.5
K	2.03-2.37	74	1.2	1.0e5	75	1.6	2.00-2.40	73	2.0	1.3e5	73	2.8
K’							1.95-2.29*	70*	2.7*	1.2e5*	70*	3.8*
K_s							1.99-2.31*	72*	1.9*	1.0e5*	72*	2.8*
K_l	2.07-2.41	74	1.1	1.0e5	76	1.4						
L							3.20-3.80	63	5.2	7.5e7	61	5.7
L’	3.42-4.12	73❖	1.4❖	1.4e8❖	68❖	3.7❖	3.50-4.10	72	1.2	1.1e8	68	3.1
M							4.50-5.10	53	8.5	2.1e9	43	12.1
M’	4.55-4.79	50	7.1	4.7e8	42	10.1	4.67-4.89*	45*	7.8*	5.6e8*	38*	10.0*

Table 3 - A numerical summary of the entire analysis is listed, with entries split according to proposed vs. Barr or IRTF bandpass, and site altitude.

* IRTF bandpass used

♣ denotes ~50% transmission points in filter profile

♠ Estimate based upon Redeye measurements at CFHT

❖ MK optimized; Barr L’ is proposed as best compromise between MK and 2 km sites.